Journal of Sound and Vibration (2001) **240**(3), 467–481
doi:10.1006/jsvi.2000.3250, available online at http://www.idealibrary.com on IDEAL®

OPTIMIZATION OF VISCOELASTIC JUNCTIONS WITH REGARD TO TRANSMISSION OF WAVE ENERGY

T. NYGREN

ABB Corporate Research, SE-721 78 Västerås, Sweden

B. LUNDBERG

The Ångström Laboratory, Uppsala University, Box 534, SE-751 21 Uppsala, Sweden

AND

L.-E. ANDERSSON

Department of Mathematics, Linköping University, SE-581 83 Linköping, Sweden

(*Received* 26 *January* 2000, *and in final form* 28 *June* 2000)

Reflection, transmission and dissipation of the energy of an incident extensional wave at a linearly viscoelastic junction between two uniform and collinear linearly elastic bars are considered. The junction consists of a finite number of uniform segments of the same material and length. The optimum shape of a junction with given material, length and number of segments which maximizes the energy transmission for given input and output bars and a given incident wave of finite duration is determined numerically with the use of a quasi-Newton method. Results are presented for rectangular incident waves of different durations and 40-segment junctions of standard linear solid material. In the special case of linearly elastic material, the optimum junctions have piece-wise constant characteristic impedances with a certain number of plateaux of equal lengths. These plateaux are independent of the number of segments provided that this number is an integral multiple of the number of plateaux. The optimum viscoelastic junctions have the appearance of deformed and displaced versions of their elastic counterparts. Thus, the plateaux of the elastic junctions are increasingly deformed and displaced with increased damping and, less markedly, with decreased response time of the material. The transitions between these plateaux of a junction appear to be discontinuous, similarly as in the case of elastic material. The apparent discontinuities become less notable with increased damping of the material.

1. INTRODUCTION

The ability of elastic waves to carry energy is sometimes used in engineering applications. In percussive drilling of rock, for example, such waves serve to transport energy through a drill string to a drill bit. These waves are commonly transmitted through junctions, where some of their energy is reflected and some is dissipated. Similarly, when any structure is subjected to a load with short duration, waves are generated and transmitted to parts of the structure where they are sometimes useful and sometimes detrimental. When the waves are transmitted through junctions of various kinds, parts of their energy are reflected and other parts are dissipated due to, for example, material damping. Depending on the application, it is sometimes desirable either to minimize or to maximize the transmission of wave energy through a junction.

0022-460X/01/080467 + 15 $35.00/0

A number of papers have dealt with the transmission of waves through junctions and maximization of the energy transmission either by optimizing the shape of the incident wave or by optimizing the junction. Early work concerning wave propagation in non-uniform elastic bars was carried out by Donnell [1]. Some general results for elastic junctions were obtained by Andersson and Lundberg [2]. Wave propagation in non-uniform viscoelastic bars was studied by Mao and Rader [3]. The possibility that different junctions may have the same transmission properties was investigated in the elastic case by Nygren *et al.* [4]. A related problem in the viscoelastic case was studied by the same authors [5]. The problem of optimizing the shape of the incident wave was considered by Lundberg *et al.* [6] for elastic junctions and by Nygren *et al.* [7] for viscoelastic ones. The optimization of elastic junctions was studied by Gupta [8], who used a numerical approach. A similar problem was tackled by Konstanty and Santosa [9], who were concerned with the design of minimally reflective coatings and used a numerical time-domain approach. Recently, the optimization of elastic junctions, was treated also by Nygren *et al.* [10], who used a variational approach and showed that, for a class of incident waves with piece-wise constant amplitudes, the optimum junctions have piece-wise constant characteristic impedances with a certain number of plateaux with equal transit times.

This paper is concerned with the reflection and transmission of the energy of an incident extensional wave at a non-uniform viscoelastic junction between two uniform and collinear elastic bars. More specifically, the aim is to determine the optimum junction with given material and length, which maximizes the energy transmission for given characteristic impedances of the input and output bars and a given incident wave of finite duration. The study is restricted to junctions which consist of a finite number of uniform segments. The effects of this restriction can be relieved by choosing the number of segments to be large. The model used and the results obtained can be interpreted also for other systems such as non-uniform viscoelastic layers between extended elastic media.

First, in section 2, fundamental relations for the reflection and transmission of waves at a non-uniform viscoelastic junction will be presented, and the optimization problem to be solved will be formulated. Then, in section 3, it will be shown how the objective function can be evaluated efficiently, and the numerical optimization procedure to be used will be presented. Finally, in section 4, numerical examples will be given for incident waves of rectangular shape and junctions made of standard linear solid material.

2. FORMULATION OF THE OPTIMIZATION PROBLEM

Consider first the propagation of extensional waves in a straight non-uniform linearly viscoelastic bar with cross-sectional area A, density ρ and complex modulus E. The quantities A and ρ are functions of the axial co-ordinate x, while E is a function of x and the angular frequency ω. It is assumed that the viscoelastic material can be represented by a series combination of Kelvin elements (spring and dashpot in parallel) or a parallel combination of Maxwell elements (spring and dashpot in series). It is also assumed in each of these cases that one spring-dashpot element is degenerated into a spring. For such a material, the relationship between stress σ and strain ε can be expressed by $P\sigma = Q\varepsilon$, where P and Q are linear differential operators with real coefficients [11]. Furthermore, because of this form of the constitutive relationship, the complex modulus can be expressed as the product

$$E(x, \omega) = E^{\infty}(x)G^2(x, \omega), \tag{1}$$

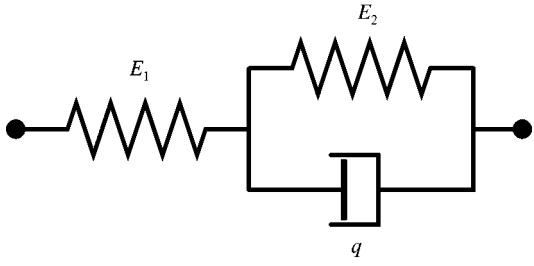

Figure 1. Standard linear solid.

where $E^\infty(x)$ is real and finite, $G(x, -\omega) = \overline{G(x, \omega)}$ (complex conjugate) and $G(x, \omega) \to 1$ as $\omega \to \infty$. In particular, $G(x, \omega) = 1$ in portions of the bar where the material is linearly elastic. It follows that the wave speed $c = (E/\rho)^{1/2}$ and the characteristic impedance $Z = A(E\rho)^{1/2}$ can be expressed as the products

$$c(x, \omega) = c^\infty(x)G(x, \omega), \quad Z(x, \omega) = Z^\infty(x)G(x, \omega), \tag{2}$$

where $c^\infty = (E^\infty/\rho)^{1/2}$ and $Z^\infty = A(E^\infty\rho)^{1/2}$ are real and finite.

For the standard linear solid shown in Figure 1, which will be considered in the numerical examples, the complex modulus is

$$E = E^\infty \frac{t_r}{t_c} \frac{1 + \mathrm{i}\omega t_c}{1 + \mathrm{i}\omega t_r}, \tag{3}$$

where $E^\infty = E_2$, and $t_c = q/E_1$ and $t_r = q/(E_1 + E_2)$ are time constants for creep and relaxation.

Wave propagation in the bar is governed by the linear system of equations

$$\frac{\partial}{\partial x}\begin{bmatrix} \hat{f} \\ \hat{v} \end{bmatrix} = \frac{\mathrm{i}\omega}{c}\begin{bmatrix} 0 & Z \\ 1/Z & 0 \end{bmatrix}\begin{bmatrix} \hat{f} \\ \hat{v} \end{bmatrix}, \tag{4}$$

where $f(x, t)$ is the normal force, positive in tension, and $v(x, t)$ is the particle velocity, positive in the direction of increasing x. The functions $\hat{f}(x, \omega)$ and $\hat{v}(x, \omega)$ are the Fourier transforms of $f(x, t)$ and $v(x, t)$; i.e., $\hat{f}(x, \omega) = \int_{-\infty}^{\infty} f(x, t)\, \mathrm{e}^{-\mathrm{i}\omega t}\, \mathrm{d}t$, and similarly for v.

Consider next a non-uniform viscoelastic junction between two semi-infinite elastic bars as shown in Figure 2. The junction occupies $\xi \in [0, d]$, where $\xi = \int_0^x \mathrm{d}s/c^\infty(s)$ is the travel time of a wave front from the origin to x, and consists of N uniform segments with different cross-sectional areas but with the same material and equal transit times $h = d/N$. The points $\xi_k = (k - 1/2)h$, $k = 0, 1, \ldots, N + 1$ are introduced; i.e., the point $\xi_0 = -h/2$ at the end of the input bar, the mid-points $\xi_1, \xi_2, \cdots, \xi_N$ of each segment, and the point $\xi_{N+1} = d + h/2$ at the beginning of the output bar. The segments of the viscoelastic junction are represented by the functions $G_1(\omega) \equiv G_2(\omega) \equiv \cdots \equiv G_N(\omega) \equiv G(\omega)$, the wave-front speeds $c_1^\infty = c_2^\infty = \cdots = c_N^\infty = c^\infty$, and the characteristic impedances at high frequencies $Z_1^\infty, Z_2^\infty, \ldots, Z_N^\infty$. Similarly, the elastic input and output bars are represented by $G_0(\omega) \equiv G_{N+1}(\omega) \equiv 1$, $c_0^\infty = c_{N+1}^\infty$, $Z_0^\infty = Z_{IN}$ and $Z_{N+1}^\infty = Z_{OUT}$.

For the segment k in the interval $(\xi_k - h/2, \xi_k + h/2)$, equation (4) gives

$$\begin{bmatrix} \hat{f} \\ \hat{v} \end{bmatrix} = \begin{bmatrix} 1 & 1 \\ -1/Z_k & 1/Z_k \end{bmatrix}\begin{bmatrix} \hat{f}_k^p\, \mathrm{e}^{-\mathrm{i}\omega(\xi - \xi_k)/G_k} \\ \hat{f}_k^n\, \mathrm{e}^{\mathrm{i}\omega(\xi - \xi_k)/G_k} \end{bmatrix}, \tag{5}$$

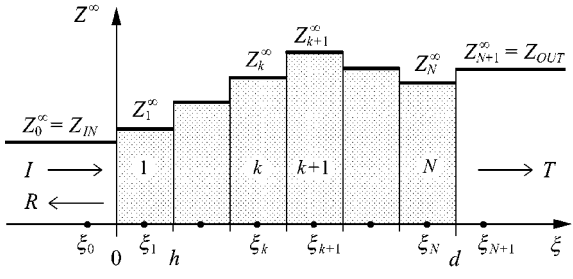

Figure 2. Viscoelastic junction with N segments between elastic bars.

where $\hat{f}_k^p(\omega)$ and $\hat{f}_k^n(\omega)$ represent forces at $\xi = \xi_k$ associated with waves travelling in the directions of increasing and decreasing ξ. With the requirement of continuity of force and particle velocity at $\xi = \xi_k + h/2 = \xi_{k+1} - h/2$, this relation and its counterpart for segment $k + 1$ give

$$\hat{\mathbf{F}}_k = \mathbf{C}_k \hat{\mathbf{F}}_{k+1}, \tag{6}$$

where

$$\hat{\mathbf{F}}_k = Z_k^{-1/2} \begin{bmatrix} \hat{f}_k^p \\ \hat{f}_k^n \end{bmatrix} \tag{7}$$

and

$$\mathbf{C}_k = \begin{bmatrix} \cosh(\alpha_k)\, \mathrm{e}^{\mathrm{i}\omega h(1/G_k + 1/G_{k+1})/2} & \sinh(\alpha_k)\, \mathrm{e}^{\mathrm{i}\omega h(1/G_k - 1/G_{k+1})/2} \\ \sinh(\alpha_k)\, \mathrm{e}^{-\mathrm{i}\omega h(1/G_k - 1/G_{k+1})/2} & \cosh(\alpha_k)\, \mathrm{e}^{-\mathrm{i}\omega h(1/G_k + 1/G_{k+1})/2} \end{bmatrix}, \tag{8}$$

with $\alpha_k = (1/2)\ln(Z_{k+1}/Z_k)$. For $k = 1, 2, \ldots, N-1$, the exponential functions in equation (8) reduce to $\mathrm{e}^{\pm \mathrm{i}\omega h/G}$ and 1.

Repeated use of equation (6) gives

$$\hat{\mathbf{F}}_0 = \mathbf{H}\hat{\mathbf{F}}_{N+1}, \quad \mathbf{H} = \mathbf{C}_0\mathbf{C}_1 \cdots \mathbf{C}_{N-1}\mathbf{C}_N, \tag{9}$$

where $\mathbf{H}$ is a transfer matrix which relates the vector $\hat{\mathbf{F}}_0$ at the input end $\xi = \xi_0$ to the vector $\hat{\mathbf{F}}_{N+1}$ at the output end $\xi = \xi_{N+1}$. These vectors can be written as

$$\hat{\mathbf{F}}_0 = Z_{IN}^{-1/2} \begin{bmatrix} \hat{f}_I \\ \hat{f}_R \end{bmatrix} = \begin{bmatrix} \hat{F}_I \\ \hat{F}_R \end{bmatrix}, \quad \hat{\mathbf{F}}_{N+1} = Z_{OUT}^{-1/2} \begin{bmatrix} \hat{f}_T \\ 0 \end{bmatrix} = \begin{bmatrix} \hat{F}_T \\ 0 \end{bmatrix}, \tag{10}$$

where $\hat{f}_I = \hat{f}_0^p$, $\hat{f}_R = \hat{f}_0^n$ and $\hat{f}_T = \hat{f}_{N+1}^p$ are the forces associated with the incident and reflected waves in the input bar, and with the transmitted wave in the output bar.

With the use of equations (9) and (10), the reflected and transmitted waves can be expressed in terms of the incident wave as

$$\hat{F}_R = (H_{21}/H_{11})\, \hat{F}_I, \quad \hat{F}_T = (1/H_{11})\, \hat{F}_I, \tag{11}$$

where $H_{11}(\omega)$ and $H_{21}(\omega)$ are the elements of transfer matrix $\mathbf{H}$.

The energies carried by the incident, reflected and transmitted waves are

$$W_I = \int_{-\infty}^{\infty} F_I^2 \, \mathrm{d}t, \quad W_R = \int_{-\infty}^{\infty} F_R^2 \, \mathrm{d}t, \quad W_T = \int_{-\infty}^{\infty} F_T^2 \, \mathrm{d}t, \tag{12}$$

and the dissipated energy is

$$W_D = W_I - (W_T + W_R). \tag{13}$$

Use of equations (11)–(13) and Parseval's identity gives the energy reflection and transmission coefficients

$$\eta_R = W_R/W_I = \int_{-\infty}^{\infty} \hat{k}_R |\hat{F}_I|^2 \, \mathrm{d}\omega \Big/ \int_{-\infty}^{\infty} |\hat{F}_I|^2 \, \mathrm{d}\omega$$

$$\eta_T = W_T/W_I = \int_{-\infty}^{\infty} \hat{k}_T |\hat{F}_I|^2 \, \mathrm{d}\omega \Big/ \int_{-\infty}^{\infty} |\hat{F}_I|^2 \, \mathrm{d}\omega \tag{14}$$

and the energy dissipation coefficient

$$\eta_D = W_D/W_I = 1 - (\eta_T + \eta_R), \tag{15}$$

where

$$\hat{k}_R = |H_{21}/H_{11}|^2, \quad \hat{k}_T = |1/H_{11}|^2. \tag{16}$$

The relation $G(-\omega) = \overline{G(\omega)}$ and equations (2), (8) and (9) give $\mathbf{C}_k(-\omega) = \overline{\mathbf{C}_k(\omega)}$ and $\mathbf{H}(-\omega) = \overline{\mathbf{H}(\omega)}$. It follows from equations (16) that $\hat{k}_R(-\omega) = \hat{k}_R(\omega)$, and similarly for $\hat{k}_T(\omega)$. Thus, $\hat{k}_R(\omega)$ and $\hat{k}_T(\omega)$ are even functions.

For given input and output characteristic impedances Z_{IN} and Z_{OUT}, material of the junction (represented by $E(\omega) = E^\infty G^2(\omega)$ and ρ), length of the junction (represented by the transit time d), number of segments N and incident wave F_I of finite duration λ ($F_I(t) = 0$ for $t \notin [0, \lambda]$), the characteristic impedances $Z_k(\omega) = Z_k^\infty G(\omega)$, $k = 1, 2, \ldots, N$, which maximize the energy transmission coefficient η_T will be sought. Thus, the following optimization problem is posed:

Given Z_{IN}, Z_{OUT}, $G(\omega)$, d, N and $F_I(t)$; find $\{Z_k^\infty\}_{k=1}^N$ such that

$$\varphi = 1 - \eta_T \text{ is minimized.}$$

As $Z_k^\infty = A_k (E^\infty \rho)^{1/2}$, this problem is equivalent to that of determining the cross-sectional areas $\{A_k\}_{k=1}^N$ which maximize the energy transmission coefficient, i.e., the optimum shape of the junction.

3. NUMERICAL OPTIMIZATION PROCEDURE

The optimization problem is solved here by numerically minimizing the objective function $\varphi(Z_1^\infty, Z_2^\infty, \ldots, Z_N^\infty)$. As there is no obvious way to express the gradients of this function analytically, these gradients are calculated numerically by the use of finite differences. This implies repeated evaluations of the objective function, and therefore it is important to calculate the energy transmission coefficient $\eta_T(Z_1^\infty, Z_2^\infty, \ldots, Z_N^\infty)$ efficiently.

For convenience, it is assumed that the incident wave has unit energy $W_I = 1$ so that $\int_{-\infty}^{\infty} |\hat{F}_I|^2 \, \mathrm{d}\omega = 2\pi$ and

$$\eta_T = (1/2\pi) \int_{-\infty}^{\infty} \hat{k}_T |\hat{F}_I|^2 \, \mathrm{d}\omega. \tag{17}$$

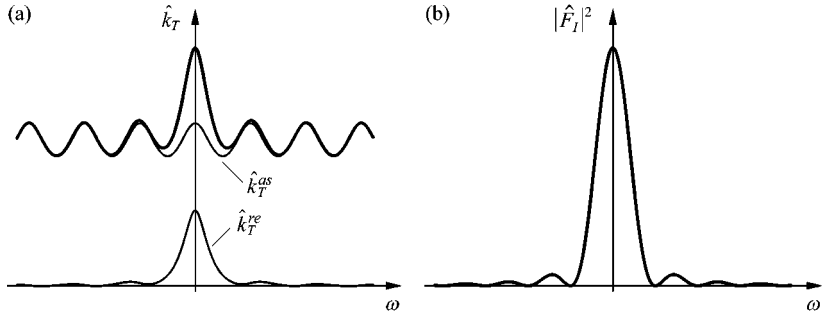

Figure 3. Character of functions involved in the integral for the energy transmission coefficient η_T. (a) The function $\hat{k}_T(\omega)$ decomposed into the asymptotic part $\hat{k}_T^{as}(\omega)$ and the remaining part $\hat{k}_T^{re}(\omega)$. (b) Spectrum $|\hat{F}_I(\omega)|^2$ of rectangular incident wave $F_I(t)$.

It is possible to evaluate this expression directly by numerical integration. However, the integrand generally decreases rather slowly with ω. Therefore, the function $\hat{k}_T(\omega)$ is instead decomposed into an asymptotic part $\hat{k}_T^{as}(\omega)$ and a remaining part $\hat{k}_T^{re}(\omega)$ so that

$$\hat{k}_T = \hat{k}_T^{as} + \hat{k}_T^{re}, \tag{18}$$

where $\hat{k}_T^{as}(\omega) - \hat{k}_T(\omega) \to 0$ and $\hat{k}_T^{re}(\omega) \to 0$ as $\omega \to \infty$. This is illustrated in Figure 3, which shows the functions $\hat{k}_T(\omega)$, $\hat{k}_T^{as}(\omega)$, $\hat{k}_T^{re}(\omega)$ and also $|\hat{F}_I(\omega)|^2$. With the use of this decomposition and equation (17), the energy transmission coefficient can be expressed as

$$\eta_T = \eta_T^{as} + \eta_T^{re}, \tag{19}$$

with

$$\eta_T^{as} = (1/2\pi)\int_{-\infty}^{\infty} \hat{k}_T^{as}|\hat{F}_I|^2 \, \mathrm{d}\omega, \quad \eta_T^{re} = (1/2\pi)\int_{-\infty}^{\infty} \hat{k}_T^{re}|\hat{F}_I|^2 \, \mathrm{d}\omega. \tag{20}$$

Consider now the first of these relations. In order to facilitate the integration, use will be made of the fact that $\hat{k}_T^{as}(\omega)$ is periodic. This periodicity can be shown as follows. From equations (1) and (3), the term $\mathrm{i}\omega h/G_k$ in the exponents of equation (8) is equal to $\mathrm{i}\omega h$ for $k = 0$ and $N + 1$, and has the expansion

$$\mathrm{i}\omega h/G_k = \mathrm{i}\omega h + \beta h + O(1/\mathrm{i}\omega) \tag{21}$$

with

$$\beta = (t_c - t_r)/2t_c t_r \tag{22}$$

for $k = 1, 2, \ldots, N$. With the use of this expansion it can be verified that $\mathbf{C}_k(\omega) - \mathbf{C}_k^{as}(\omega) \to 0$ as $\omega \to \infty$, where

$$\mathbf{C}_k^{as} = \begin{bmatrix} \cosh(\alpha_k^\infty)\, \mathrm{e}^{(\beta_k + \beta_{k+1})h/2} \mathrm{e}^{\mathrm{i}\omega h} & \sinh(\alpha_k^\infty)\, \mathrm{e}^{(\beta_k - \beta_{k+1})h/2} \\ \sinh(\alpha_k^\infty)\, \mathrm{e}^{-(\beta_k - \beta_{k+1})h/2} & \cosh(\alpha_k^\infty)\, \mathrm{e}^{-(\beta_k + \beta_{k+1})h/2} \mathrm{e}^{-\mathrm{i}\omega h} \end{bmatrix}, \tag{23}$$

$\alpha_k^\infty = (1/2)\ln(Z_{k+1}^\infty/Z_k^\infty)$, $\beta_1 = \beta_2 = \cdots = \beta_N = \beta$, and $\beta_0 = \beta_{N+1} = 0$. As this matrix is periodic with period $2\pi/h$, the matrix

$$\mathbf{H}^{as} = \mathbf{C}_0^{as}\mathbf{C}_1^{as} \cdots \mathbf{C}_{N-1}^{as}\mathbf{C}_N^{as} \tag{24}$$

is also periodic with the same period. Also, it follows from equations (9) and (24) that $\mathbf{H}(\omega) - \mathbf{H}^{as}(\omega) \to 0$ as $\omega \to \infty$. Thus, it follows from equation (16) that

$$\hat{k}_T^{as} = |1/H_{11}^{as}|^2. \tag{25}$$

It can be shown by induction that the element H_{11}^{as} is a trigonometric polynomial $e^{i\omega h} \Sigma_{k=0}^{N} a_k e^{i\omega h(N-2k)}$ with real coefficients a_k [2]. Thus, $|H_{11}^{as}|^2$ is a linear combination of the functions $\{e^{i\omega 2hk}\}_{k=-N}^{N}$. Therefore, equation (25) shows that $\hat{k}_T^{as}$ is periodic with period $2\pi/2h$ and can be expanded in the Fourier series

$$\hat{k}_T^{as}(\omega) = \sum_{m=-\infty}^{\infty} \kappa_m^{as} e^{im2h\omega} = \sum_{m=-\infty}^{\infty} \kappa_m^{as} e^{-i\omega 2mh} \tag{26}$$

with Fourier coefficients

$$\kappa_m^{as} = \kappa_{-m}^{as} = \frac{h}{\pi} \int_{-\pi/2h}^{\pi/2h} \hat{k}_T^{as}(\omega)\, e^{-im2h\omega}\, d\omega, \tag{27}$$

where use has been made of the fact that $\hat{k}_T^{as}(\omega)$ is even. By inversion,

$$k_T^{as}(t) = \sum_{m=-\infty}^{\infty} \kappa_m^{as} \delta(t - 2mh), \tag{28}$$

where $\delta(t)$ is the delta function.

By use of equation (17), Parseval's identity and $\overline{\hat{F}_I(\omega)} = \hat{F}_I(-\omega)$,

$$\eta_T^{as} = \int_{-\infty}^{\infty} k_T^{as}(t) g(t)\, dt, \tag{29}$$

where

$$g(t) = \int_{-\infty}^{\infty} F_I(t+u) F_I(u)\, du. \tag{30}$$

Clearly, $g(t) = 0$ for $t \notin [-\lambda, \lambda]$, as $F_I(t) = 0$ for $t \notin [0, \lambda]$. Substitution of equation (28) into (29) gives

$$\eta_T^{as} = \sum_{m=-Q}^{Q} \kappa_m^{as} g_m = \kappa_0^{as} g_0 + 2 \sum_{m=1}^{Q} \kappa_m^{as} g_m, \tag{31}$$

where $g_m = g(2mh)$, and Q is the integer part of $\lambda/2h$. Here, use has also been made of the relations $g_{-m} = g_m$ and $\kappa_{-m}^{as} = \kappa_m^{as}$. The Fourier coefficients κ_m^{as} are obtained from the function $\hat{k}_T^{as}(\omega)$ by using the fast fourier transform.

Consider next the second part of equations (20) which involves the function $\hat{k}_T^{re} = \hat{k}_T - \hat{k}_T^{as}$. As the integrand is an even function (which follows from the relations $\hat{k}_T^{re}(-\omega) = \hat{k}_T^{re}(\omega)$ and $\hat{F}_I(-\omega) = \overline{\hat{F}_I(\omega)}$), it is sufficient to consider positive values of ω. Also, as illustrated by Figure 3, the integrand generally decreases rapidly towards zero as ω grows. Therefore, the integration can be carried out numerically with use of the trapezoidal rule. The lower limit of integration is taken as zero and the upper limit is chosen adaptively with regard to the desired accuracy.

A quasi-Newton method with BFGS update of the Hessian matrix $\mathbf{B} = \nabla^2\varphi$ [12] is used to minimize the objective function $\varphi(\mathbf{z})$ with $\mathbf{z} = (Z_1^\infty, Z_2^\infty, \ldots, Z_N^\infty)^{\mathrm{T}}$. The elements of $\mathbf{z}$ are normalized so that $Z_{IN} = 1$. The kth iteration of $\mathbf{z}$ is

$$\mathbf{z}_{k+1} = \mathbf{z}_k + \gamma_k \mathbf{d}_k, \quad \mathbf{d}_k = -\mathbf{B}_k^{-1}\nabla\varphi(\mathbf{z}_k), \tag{32}$$

where $\nabla\varphi$ is the gradient of the objective function φ. Line search in the direction $\mathbf{d}_k$ (i.e., finding the value γ_k which minimizes $\varphi(\mathbf{z}_k + \gamma_k\mathbf{d}_k)$) is carried out by a mixed quadratic and cubic interpolation. The BFGS update is

$$\mathbf{B}_{k+1} = \mathbf{B}_k + \frac{\mathbf{q}_k\mathbf{q}_k^{\mathrm{T}}}{\mathbf{q}_k^{\mathrm{T}}\mathbf{p}_k} - \frac{\mathbf{B}_k\mathbf{p}_k\mathbf{p}_k^{\mathrm{T}}\mathbf{B}_k}{\mathbf{p}_k^{\mathrm{T}}\mathbf{B}_k\mathbf{p}_k}, \tag{33}$$

where

$$\mathbf{p}_k = \mathbf{z}_{k+1} - \mathbf{z}_k, \quad \mathbf{q}_k = \nabla\varphi(\mathbf{z}_{k+1}) - \nabla\varphi(\mathbf{z}_k). \tag{34}$$

Normally, the initial vector $\mathbf{z}_0$ is taken as the solution of the corresponding elastic problem [10]. The initial Hessian is taken to be $\mathbf{B}_0 = \mathbf{I}$. The iteration is stopped when $\max(|\mathbf{d}_k|) < 2\times10^{-6}$ and $-\nabla\varphi(\mathbf{z}_k)^{\mathrm{T}}\mathbf{d}_k < 2\times10^{-6}$. These criteria concern the changes in $\mathbf{z}$ and in φ, respectively, from one step of iteration to the next.

When the optimum junction and the energy transmission coefficient η_T are known, the energy reflection coefficient η_R can be determined from equations (14), in a similar way as η_T; and the energy dissipation coefficient η_D can be obtained from equation (15).

4. NUMERICAL EXAMPLES

In the numerical examples which follow, the ratio between the characteristic impedances of the output and input bars is taken to be $Z_{OUT}/Z_{IN} = 2$, and the number of segments of each junction is chosen to be $N = 40$.

The material is represented by the standard linear solid model, i.e., equation (3). For this model, the loss angle $\delta = \arctan[\mathrm{Im}(E)/\mathrm{Re}(E)]$ has the maximum

$$\delta_0 = \arctan[(t_c - t_r)/2(t_c t_r)^{1/2}] \tag{35}$$

at $\omega = 1/t_0$ with

$$t_0 = (t_c t_r)^{1/2}. \tag{36}$$

The incident wave is chosen to be a rectangular pulse with duration λ.

Figures 4–6 show the characteristic impedances $\{Z_k^\infty\}_{k=1}^N$ of optimum junctions for the normalized incident wave durations $\lambda/2d = \frac{1}{10}, \frac{1}{5}, \frac{1}{2}$, 1 and 2, and the maximum loss angles $\delta_0 = 0^\circ$, 15° and 45°. Figure 4 shows results for the normalized response time constant $t_0/2d = 0{\cdot}5$, Figure 5 for $t_0/2d = 1$, and Figure 6 for $t_0/2d = 2$.

Figure 7 shows the energy reflection, transmission and dissipation coefficients η_R, η_T and η_D for optimum junctions versus the normalized incident wave duration $\lambda/2d$. Results are shown for the maximum loss angles $\delta_0 = 0^\circ$, 15° and 45°, and for the normalized response time parameters $t_0/2d = 0{\cdot}5$, 1 and 2.

The numerical method used does not guarantee that the maximum of the energy transmission coefficient η_T found in each numerical example is not just one of the several

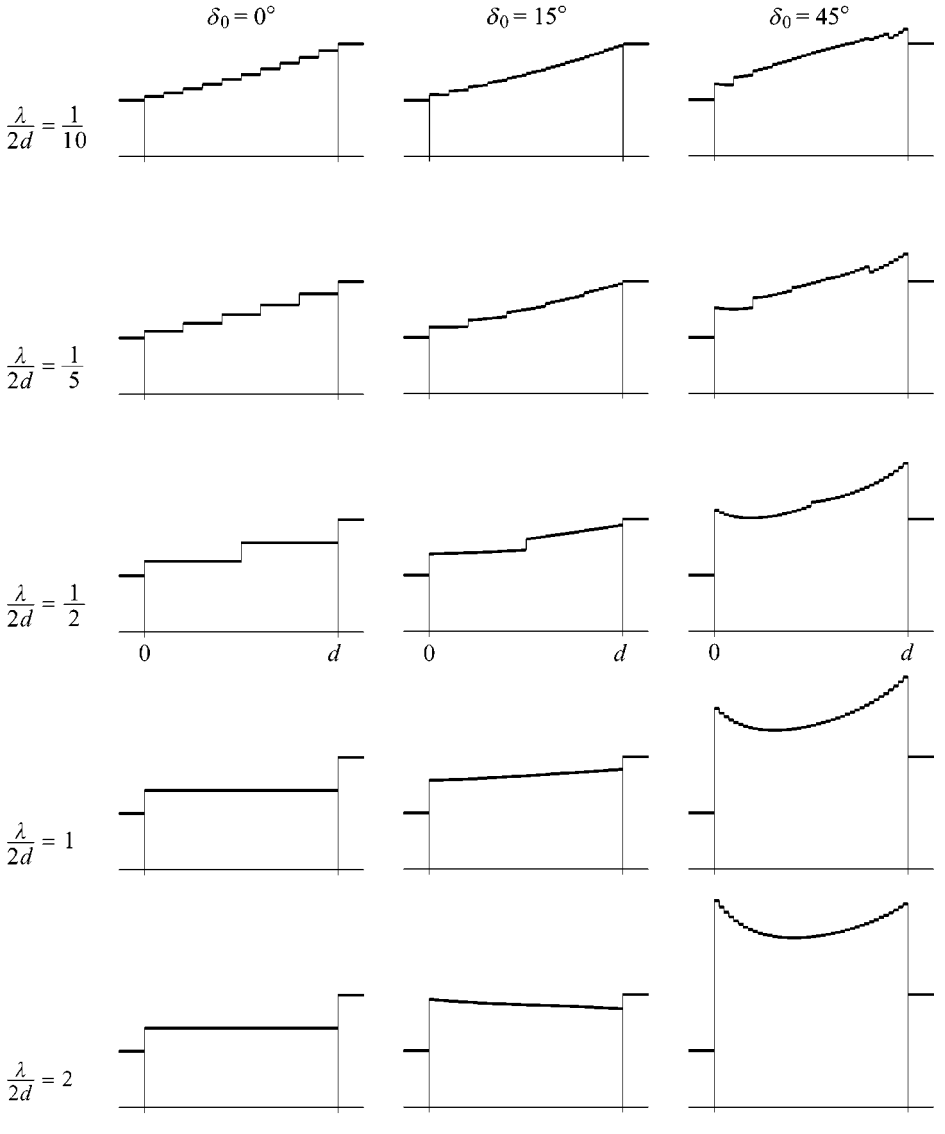

Figure 4. Characteristic impedances $\{Z_k^{\infty}\}_{k=1}^{N}$ of optimum junctions for rectangular incident waves with different normalized durations $\lambda/2d$ and different values of the maximum loss angle δ_0. Characteristic impedance ratio $Z_{OUT}/Z_{IN} = 2$, normalized response time parameter $t_0/2d = 0{\cdot}5$ and number of segments $N = 40$.

local maxima. However, numerical experiments carried out with different initial vectors $\mathbf{z}_0$ never changed the result of an optimization which indicates that the maxima obtained are global.

5. DISCUSSION

The governing system of equations (4) is based on the assumption that the normal stress associated with the waves in the input bar, the junction and the output bar is uniformly distributed and that the state of stress is uni-axial. However, the axial expansions and

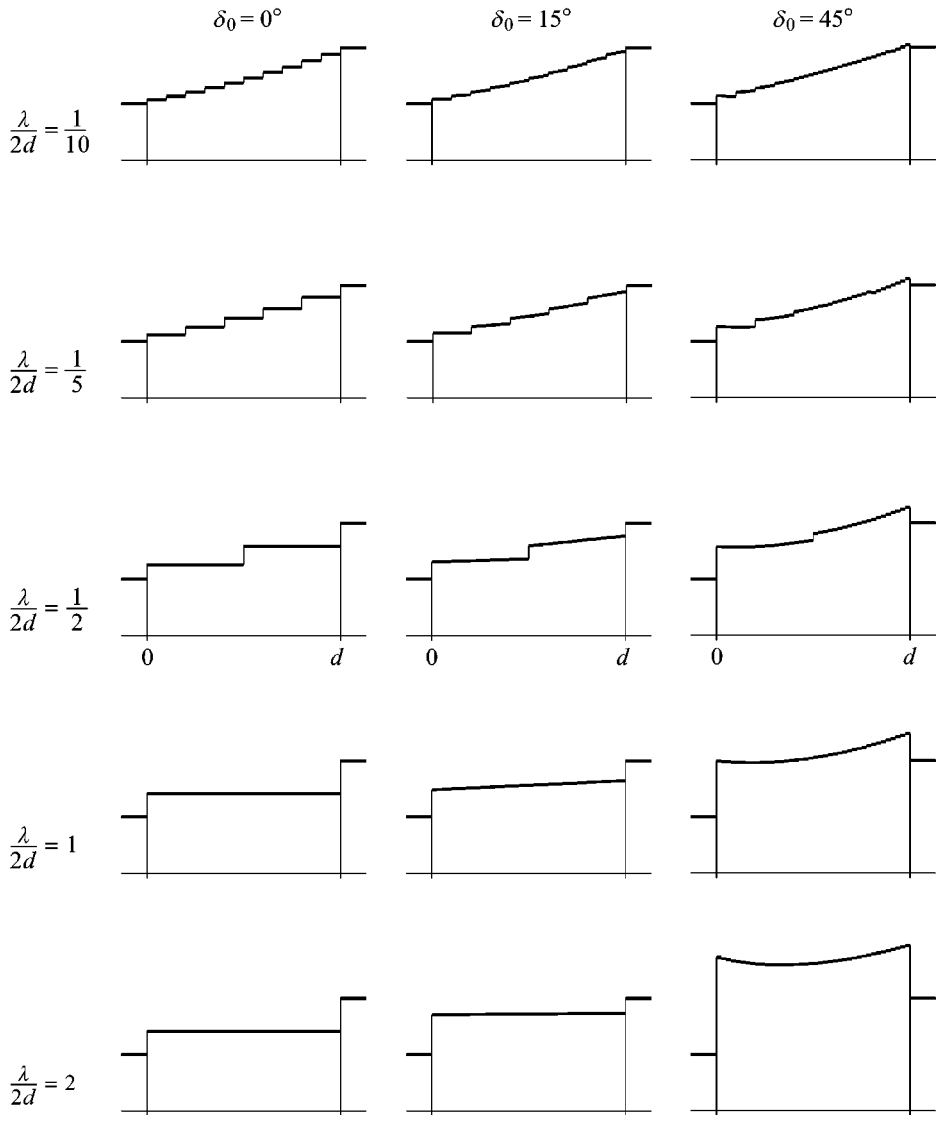

Figure 5. Characteristic impedances $\{Z_k^\infty\}_{k=1}^N$ of optimum junctions for rectangular incident waves with different normalized durations $\lambda/2d$ and different values of the maximum loss angle δ_0. Characteristic impedance ratio $Z_{OUT}/Z_{IN} = 2$, normalized response time parameter $t_0/2d = 1$ and number of segments $N = 40$.

contractions associated with the waves give rise to lateral motions which necessarily result in non-uniform distributions and three-axial states of stress. These and other three-dimensional (3D) effects are important only if the operative wavelengths are of the same order as the transverse dimensions of the bars and the junction or less [13]. For the validity of the results, therefore, it is a necessary requirement that the incident wave be much longer, say, by a factor of 10 or more, than these transverse dimensions.

When the parameter $\delta_0 = 0^\circ$, it follows from equation (35) that $t_c = t_r$. Also, it follows from equation (3) that $E = E^\infty = E_2$. Thus in this case the complex modulus is real and constant, which means that the junction is linearly elastic. For $0^\circ < \delta_0 < 90^\circ$, the junction is linearly viscoelastic, and the damping of the material increases with δ_0. The parameter

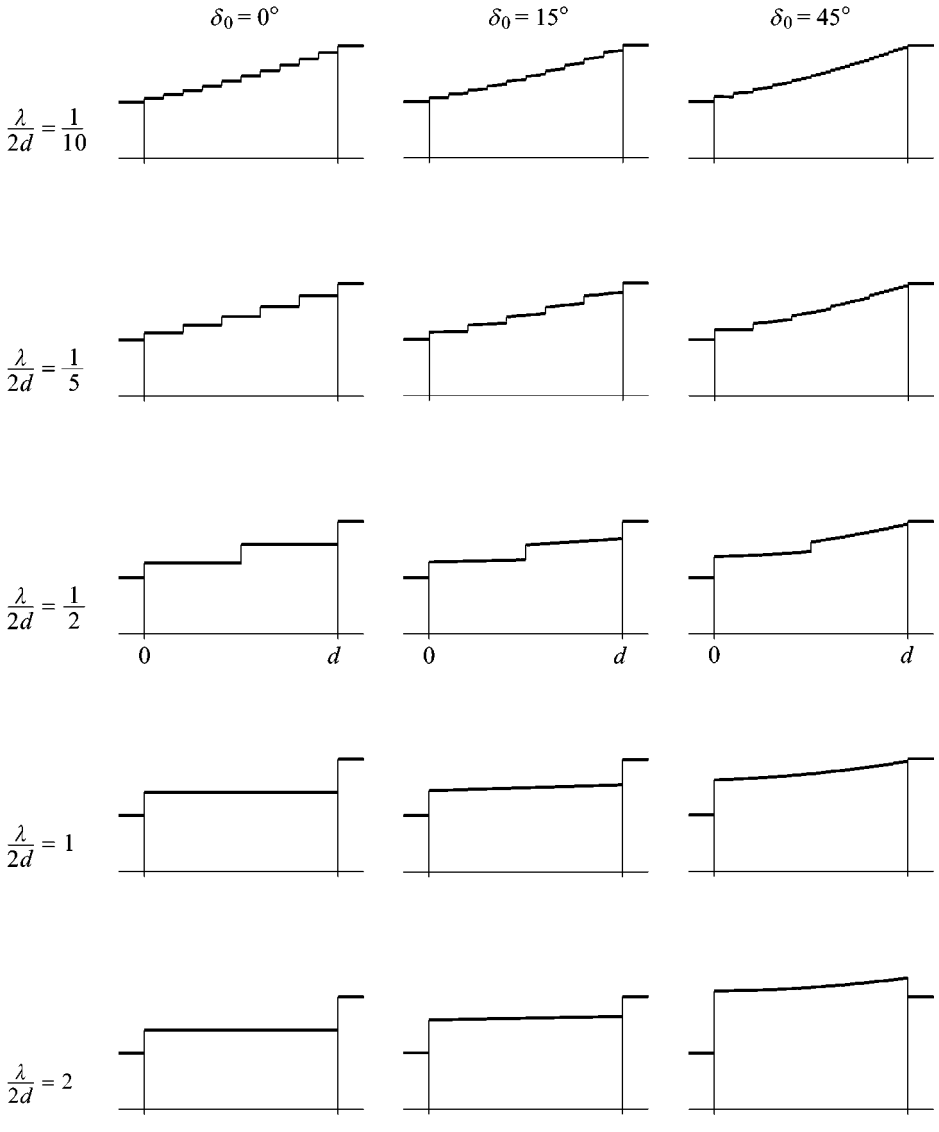

Figure 6. Characteristic impedances $\{Z_k^\infty\}_{k=1}^N$ of optimum junctions for rectangular incident waves with different normalized durations $\lambda/2d$ and different values of the maximum loss angle δ_0. Characteristic impedance ratio $Z_{OUT}/Z_{IN} = 2$, normalized response time parameter $t_0/2d = 2$ and number of segments $N = 40$.

t_0 is the geometrical mean of the time constants t_c for creep and t_r for relaxation which characterize the response of the viscoelastic material to abrupt changes of stress and strain respectively. Therefore, the parameter t_0 represents these response times of the viscoelastic material, and in this sense it is considered here to be a response time parameter itself.

The optimum elastic junctions shown in Figures 4–6 for $\delta_0 = 0°$ and $\lambda/2d$ in the range $\frac{1}{10}$–2 have piece-wise constant characteristic impedances with plateaux in agreement with [10]. Thus, when $\lambda/2d = m/n$, where m and n are integers without common factor, the optimum junction has n plateaux regardless of the number of segments N used to represent it provided that N is an integral multiple of n. Also, the optimum elastic junctions are

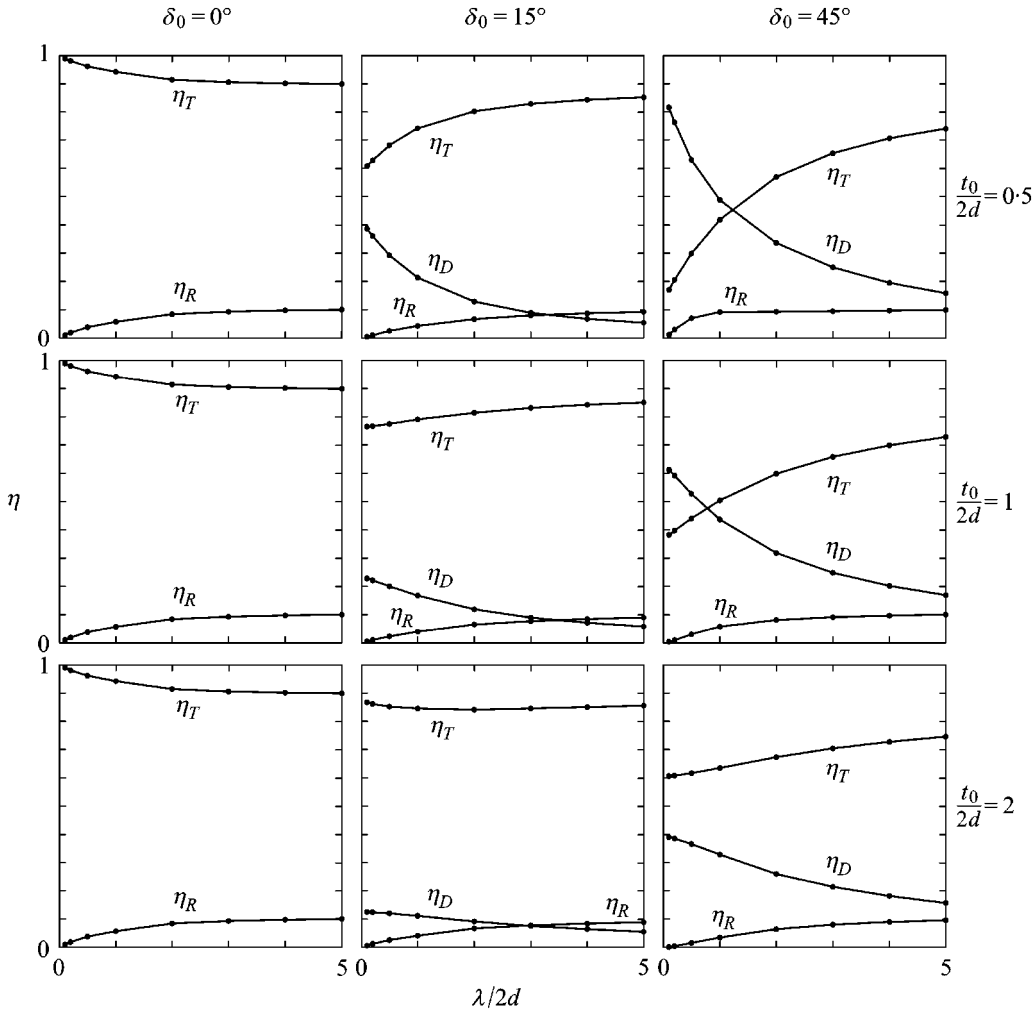

Figure 7. Energy reflection, transmission and dissipation coefficients η_R, η_T and η_D for optimum junctions versus normalized duration $\lambda/2d$ of rectangular incident wave for different values of the maximum loss angle δ_0 and the normalized response time parameter $t_0/2d$. Characteristic impedance ratio $Z_{OUT}/Z_{IN} = 2$ and number of segments $N = 40$.

anti-symmetric in the sense that $Z_1 Z_N = Z_2 Z_{N-1} = \cdots = Z_{IN} Z_{OUT}$ [2]. This property of optimum junctions was observed also by Konstanty and Santosa [9] from their numerical results for pulses of small width. Finally, it can be noticed, in agreement with [10], that for the shortest incident wave in Figure 4 ($\lambda/2d = \frac{1}{10}$) and elastic material ($\delta_0 = 0°$), the characteristic impedance ratios $\{Z_k/Z_{k+1}\}_{k=0}^{N}$ are approximately constant. Thus, in this case, the characteristic impedances are in approximate geometrical progression. This indicates that for very short incident waves, the optimum elastic junction would have exponential variation of its characteristic impedance.

Figures 4–6 show that the optimum viscoelastic junctions ($\delta_0 = 15$ and $45°$) have the appearance of deformed versions of their elastic counterparts ($\delta_0 = 0°$). Thus, the plateaux of the elastic junctions are increasingly deformed and displaced with increased damping parameter δ_0 and, less markedly, with decreased response time parameter $t_0/2d$. Also, the transitions between these deformed plateaux of a junction appear to be discontinuous,

similar to the elastic case. However, the apparent discontinuities become decreasingly notable with increased damping.

It may appear strange that the optimum viscoelastic junctions shown in Figures 4–6 for $\delta_0 = 45^\circ$ and $\lambda/2d = 2$ have characteristic impedances $\{Z_k^\infty\}_{k=1}^N$ which are larger than the input and output characteristic impedances Z_{IN} and Z_{OUT}. This means that the masses $\int Z^\infty(\xi)\,\mathrm{d}\xi$ of these junctions are large (relative to the mass of a portion of the input bar with the same transit time d as the junction, which has the mass $Z_{IN}d$), which promotes reflection and, correspondingly, counteracts transmission. However, also the stiffnesses $[\int \mathrm{d}\xi/Z^\infty(\xi)]^{-1}$ of these junctions are large (relative to the stiffness of a portion of the input bar with the same transit time d as the junction, which has the stiffness Z_{IN}/d), which counteracts dissipation and, therefore, promotes transmission. Also, Figure 7 shows that in these cases $\eta_R \ll \eta_D$, i.e., the reflected energies are much smaller than the dissipated energies. Therefore, the process of optimization may have promoted transmission by decreasing dissipation at the cost of increased reflection. For relatively short incident waves (say, $\lambda/2d < 1$), however, the mass and stiffness of a junction have little relevance to the propagation of waves, and it can be seen in Figures 4–6 that in such cases the optimum viscoelastic junctions are less different from the elastic ones.

For short incident waves, with small values of $\lambda/2d$, and an elastic junction with slowly varying characteristic impedance, the energy reflection and transmission coefficients should tend to zero and unity respectively. Thus, such relatively short waves should be transmitted without being affected by the apparently slow change of characteristic impedance of the junction. For long incident waves, with large values of $\lambda/2d$ and energy spectrum close to $\omega = 0$, and an elastic or viscoelastic junction with finite characteristic impedances, the energy reflection coefficient should tend to $\eta_R^A = [(Z_{IN} - Z_{OUT})/(Z_{IN} + Z_{OUT})]^2$ and the transmission coefficient to $\eta_T^A = 4Z_{IN}Z_{OUT}/(Z_{IN} + Z_{OUT})^2$. These are the energy reflection and transmission coefficients for any incident wave when there is an abrupt change of characteristic impedance from Z_{IN} to Z_{OUT}. Thus, such relatively long waves should be transmitted as though the change in characteristic impedance was abrupt from Z_{IN} to Z_{OUT}. It follows that optimization of a viscoelastic junction can be expected to be insignificant for very large values of $\lambda/2d$.

Figure 7 shows that in the absence of damping ($\delta^\circ = 0^\circ$), the energy reflection and transmission coefficients η_R and η_T have the expected behaviour for small and large values of $\lambda/2d$. Thus, η_R asymptotically increases with $\lambda/2d$ from zero to $\eta_R^A = 0.111$, whereas η_T asymptotically decreases from unity to $\eta_T^A = 0.889$. In the presence of damping, the general behaviour of η_R is the same as in the elastic case, whereas that of η_T is different. Thus, η_T asymptotically increases or decreases with $\lambda/2d$ from a value between zero and one for small values of this parameter to η_T^A for large values. The dissipation coefficient η_D assumes a value between zero and one for small values of $\lambda/2d$ and asymptotically approaches zero for large values of this parameter. The main effects of increasing the response time parameter $t^0/2d$ are to increase the transmission coefficient η_T, to decrease the reflection coefficient η_R and to decrease the dissipation coefficient η_D.

The weak dependence of the coefficients η_R, η_T and η_D on the parameters δ_0 and $t_0/2d$ for large values of the normalized wave duration $\lambda/2d$ can be explained as follows. When the front of a rectangular incident wave arrives at a junction, waves are transmitted into the junction where they are repeatedly reflected at the two end faces. As a result, energy is dissipated. If the incident wave is sufficiently long, the reflected and transmitted waves reach constant amplitudes and the junction comes into a state of constant stress, strain and velocity. While this state prevails, the junction provides a rigid connection between the input and output bars, and its mass has no effect as there is no acceleration. Also, there is no dissipation in the junction as the strain rate is zero. Repeated reflections of waves and dissipation

in the junction resume at the arrival of the end of the incident wave. Therefore, if the incident wave is very long, reflection and transmission mostly occur as an abrupt change in characteristic impedance from Z_{IN} to Z_{OUT}.

ACKNOWLEDGMENTS

The authors are indebted to the Swedish Research Council for Engineering Sciences (TFR) for the financial support.

REFERENCES

1. L. H. DONNEL 1930 *Transactions of American Society of Mechanical Engineers* **52**, 153–167. Longitudinal wave transmission and impact.
2. L.-E. ANDERSSON and B. LUNDBERG 1984 *Wave Motion* **6**, 389–406. Some fundamental transmission properties of impedance transitions.
3. M. MAO and D. RADER 1979 *International Journal of Solids and Structures* **6**, 519–538. Longitudinal pulse propagation in nonuniform elastic and viscoelastic bars.
4. T. NYGREN, L.-E. ANDERSSON and B. LUNDBERG 1999 *Wave Motion* **30**, 143–158. Synthesis of elastic junctions with wave transmission properties of a given junction.
5. T. NYGREN, B. LUNDBERG and L.-E. ANDERSSON 1997 *Journal of Sound and Vibration* **199**, 323–336. Dissipation of energy in a viscoelastic junction between elastic bars: dependence of transmission direction.
6. B. LUNDBERG, R. GUPTA and L.-E. ANDERSSON 1979 *Wave Motion* **1**, 193–200. Optimum transmission of elastic waves through joints.
7. T. NYGREN, L.-E. ANDERSSON and B. LUNDBERG 1996 *European Journal of Mechanics A/Solids* **15**, 29–49. Optimum transmission of extensional waves through a non-uniform viscoelastic junction between elastic bars.
8. R. GUPTA 1982 *Wave Motion* **4**, 75–83. Optimum design of wave transmitting joints.
9. H. KONSTANTY and F. SANTOSA 1995 *Wave Motion* **21**, 291–309. Optimal design of minimally reflective coatings.
10. T. NYGREN, L.-E. ANDERSSON and B. LUNDBERG 1999 *Wave Motion* **29**, 223–244. Optimisation of elastic junctions with regard to transmission of wave energy.
11. W. FLÜGGE 1975 *Viscoelasticity*. Berlin: Springer-Verlag.
12. D.G. LUENBERGER 1989 *Linear and Nonlinear Programming*. Reading, MA: Addison-Wesley Publishing Company, Inc.
13. H. KOLSKY 1963 *Stress Waves in Solids*. New York: Dover Publications, Inc.

APPENDIX A: NOMENCLATURE

A	cross-sectional area
$\mathbf{C}$	transfer matrix of segment
E	complex modulus
E_1, E_2	constitutive parameters (stiffness)
$\mathbf{F}$	vector defining wave amplitudes
G	function defining frequency dependence of E, c, and Z
$\mathbf{H}$	transfer matrix of junction
$\mathbf{I}$	identity matrix
N	number of segments
W	energy
Z	characteristic impedance
c	wave speed
d	transit time through junction
f	normal force
h	transit time through segment

$\hat{k}_R, \hat{k}_T$	energy reflection and transmission coefficients for a given frequency
q	constitutive parameter (viscosity)
t	time
t_0	response time parameter of material
v	particle velocity
x	axial co-ordinate (distance)
$\mathbf{z}$	vector of characteristic impedances

Greek letters

α	logarithmic measure of characteristic impedance ratio
β	coefficient in series expansion
δ	delta function; loss angle of material
δ_0	maximum loss angle of material
η	energy coefficient
λ	duration of incident wave
ξ	axial co-ordinate (travel time)
ρ	density
φ	objective function
ω	angular frequency

Subscripts

D	dissipated
I	incident
IN	input bar
OUT	output bar
R	reflected
T	transmitted
c	creep
r	relaxation
0	maximum loss angle of material

Superscripts

A	abrupt
as	asymptotic part
n	negative direction
p	positive direction
re	remaining part
∞	high frequencies